BIOCHEMISTRY
including biophysical chemistry & molecular biology

Article

pubs.acs.org/biochemistry

Detection of Distinct α-Helical Rearrangements of Cyclobutane Pyrimidine Dimer Photolyase upon Substrate Binding by Fourier Transform Infrared Spectroscopy

I M. Mahaputra Wijaya,[†] Yu Zhang,[†] Tatsuya Iwata,[†,‡] Junpei Yamamoto,[§] Kenichi Hitomi,[∥,⊥] Shigenori Iwai,[§] Elizabeth D. Getzoff,[∥] and Hideki Kandori*,[†]

[†]Department of Frontier Materials and [‡]Center for Fostering Young and Innovative Researchers, Nagoya Institute of Technology, Showa-ku, Nagoya 466-8555, Japan

[§]Graduate School of Engineering Science, Osaka University, Toyonaka, Osaka 560-8531, Japan

[∥]Department of Integrative Structural and Computational Biology and The Skaggs Institute for Chemical Biology, The Scripps Research Institute, La Jolla, California 92037, United States

[⊥]Section of Laboratory Equipment, National Institute of Biomedical Innovation, 7-6-8, Saito-Asagi, Ibaraki, Osaka 567-0085, Japan

Supporting Information

ABSTRACT: Photolyases (PHRs) utilize near-ultraviolet (UV)−blue light to specifically repair the major photoproducts (PPs) of UV-induced damaged DNA. The cyclobutane pyrimidine dimer PHR (CPD-PHR) from *Escherichia coli* binds flavin adenine dinucleotide (FAD) as a cofactor and 5,10-methenyltetrahydrofolate as a light-harvesting pigment and specifically repairs CPD lesions. By comparison, a second photolyase known as (6−4) PHR, present in a range of higher organisms, uniquely repairs (6−4) PPs. To understand the repair mechanism and the substrate specificity that distinguish CPD-PHR from (6−4) PHR, we applied Fourier transform infrared (FTIR) spectroscopy to bacterial CPD-PHR in the presence or absence of a well-defined DNA substrate, as we have studied previously for vertebrate (6−4) PHR. PHRs show light-induced reduction of FAD, and photorepair by CPD-PHR involves the transfer of an electron from the photoexcited reduced FAD to the damaged DNA for cleaving the dimers to maintain the DNA's integrity. Here, we measured and analyzed difference FTIR spectra for the photoactivation and DNA photorepair processes of CPD-PHR. We identified light-dependent signals only in the presence of substrate. The signals, presumably arising from a protonated carboxylic acid or the DNA substrate, implicate conformational rearrangements of the protein and substrate during the repair process. Deuterium exchange FTIR measurements of CPD-PHR highlight potential differences in the photoactivation and photorepair mechanisms in comparison to those of (6−4) PHR. Although CPD-PHR and (6−4) PHR appear to exhibit similar overall structures, our studies indicate that distinct conformational rearrangements, especially in the α-helices, are initiated within these enzymes upon binding of their respective DNA substrates.

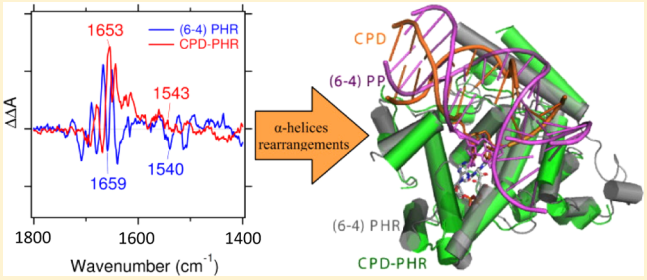

Ultraviolet light emitted from the sun causes damage to DNA by initiating the photoisomerization of two adjacent pyrimidine bases. This reaction typically results in the formation of either a cyclobutane pyrimidine dimer (CPD) or pyrimidine-(6−4)-pyrimidone photoproduct [(6−4) PP]. CPDs are more prevalent throughout nature and are highly mutagenic, while (6−4) PPs are less common; however, the presence of (6−4) PPs can be lethal because of functional group transfer (Figure 1).[1−3] Nucleotide excision repair and translesion DNA synthesis are typically responsible for UV-induced damage repair, in which various protein complexes contribute to removal of the lesion to restore fidelity within the genetic information.[4,5] On the other hand, many organisms in all three kingdoms of life possess a rapid response DNA repair enzyme that utilizes near-UV−blue light for lesion removal. This enzyme, named photolyase (PHR), can restore two native pyrimidines from a single UV-induced photoproduct by the transfer of an electron from its light-activated cofactor. To date, two types of PHRs are known on the basis of the specific lesions they repair: CPD-PHR and (6−4) PHR.[3]

PHRs bind flavin adenine dinucleotide (FAD) as a cofactor.[6,7] In addition to FAD, the 55 kDa CPD-PHR form *Escherichia coli* also binds 5,10-methenyltetrahydrofolate (MTHF) as a light-harvesting antenna.[8] However, FAD is the essential component for the catalysis of DNA repair. Indeed, the bacterial CPD-PHR is functional even without the second chromophore. The reduced form of FAD ($FADH^-$) is

Received: December 2, 2012
Revised: January 15, 2013
Published: January 21, 2013

dx.doi.org/10.1021/bi3016179 | *Biochemistry* 2013, 52, 1019−1027

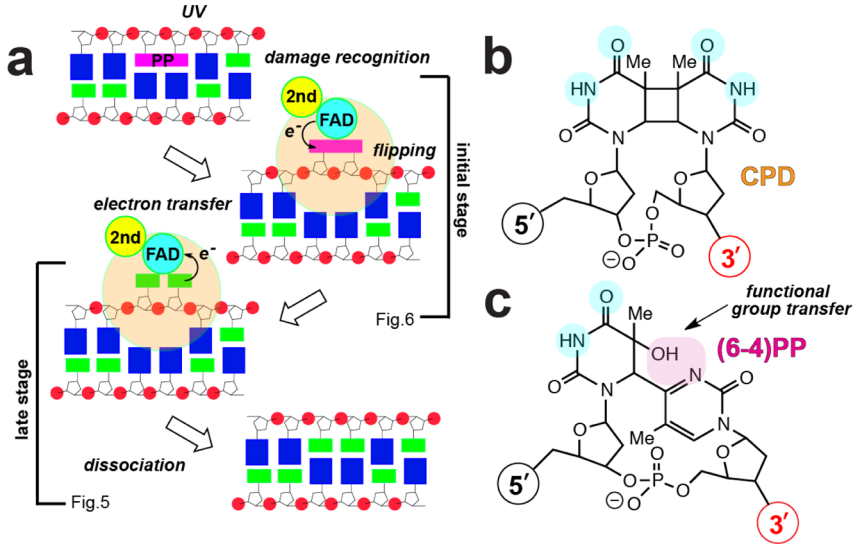

Figure 1. (a) Schematic showing the overall reaction mechanism for photorepair of UV-induced damage by PHRs. PHR (orange) light-independently recognizes PP (pink) in the DNA duplex and transfers an electron from light-excited FAD (cyan) to cleave the covalent bond(s). The redundant electron in DNA returns from the restored pyrimidine bases (green) to the FAD semiquinone form of PHR, while PHR releases the intact DNA. Purine bases are colored blue and the second chromophore of PHR yellow. UV radiation induces two major covalently linked pyrimidine dimers with different linkages and distinct features at the 3′-side. PHRs specifically recognize these dimers within the DNA duplex and light-dependently restore the original two pyrimidine bases. CPD (b) is repaired by CPD-PHR, while (6–4) PP (c) is removed by (6–4) PHRs.

responsible for the DNA repair activity of PHR, the mechanism of which is now well established.[9] An electron is transferred from the excited $FADH^-$ to the DNA substrate in a light-dependent manner (Figure 1a), leaving the cofactor in the neutral semiquinone radical state ($FADH^•$). Once the restoration of two pyrimidines is completed, an electron is transferred back from the repaired DNA to PHR, and the FAD cofactor is returned to its original fully reduced form.[10] At least in vitro, FAD of PHR is subject to oxidation, thereby intensifying the yellow color of the flavoprotein. However, the catalytically active PHR form can easily be regained by photoactivation to produce the active form or the anionic hydroquinone ($FADH^-$), via the neutral semiquinone radical ($FADH^•$) with illumination via >390 and >550 nm light. Three conserved tryptophans (W306, W356, and W382 in *E. coli* CPD-PHR) have been implicated in photoreduction of the FAD. Solvent-exposed W306 functions as a terminal electron donor, while FAD receives an electron from nearby W382. W356 mediates the electron transfer between W306 and W382.[11]

Crystallographic studies of PHRs have revealed the molecular nature of both the FAD binding and substrate recognition sites. During the repair process, the photoproduct becomes flipped out from the DNA duplex and consequently resides closer to the FAD cofactor buried inside the protein (Figure 1a).[12] These structural features are common between CPD-PHR and (6–4) PHRs despite their different photoproduct substrates. However, detailed information about how this reaction proceeds and the structural events that occur during the photorepair process are still lacking. Formation of either a CPD or (6–4) photoproduct following UV irradiation produces distinct features within the DNA strand, especially at the 3′-hydroxyl side (Figure 1b,c). The 3′-base of a (6–4) PP is distorted, losing its functional hydroxyl group for thymidine and its amino group for cytidine. By contrast, a CPD lesion retains its Watson–Crick/Hoogsteen base pair sites, but rotation of its glycosylic bonds becomes limited. Therefore, the initial damage recognition processes for CPD-PHR and (6–4) PHRs are likely to differ.

Light-induced difference Fourier transform infrared (FTIR) spectroscopy is a powerful method for studying structure–function relationships in photoreceptive proteins. Indeed, this sophisticated method has been applied successfully to various photoreceptive proteins, including rhodopsin,[13] the BLUF domain,[14] the LOV domain,[15] cryptochrome (Cry)-DASH,[16] CPD-PHR,[17] and (6–4) PHR.[18] To improve our understanding of the underlying reaction mechanisms associated with PHRs, we have improved sample preparation methods to better monitor enzyme–substrate turnover by FTIR and to increase the resolution to measure aspects of the photoactivation, photorepair, and damaged DNA binding process. Aqueous sampling allows efficient substrate consumption but often perturbs FTIR signals. Identifying a buffer condition that will suitably cover the entire PHR process is thus very challenging. By applying knowledge gained from our study of Cry-DASH and (6–4) PHR, we have successfully applied FTIR to *E. coli* CPD-PHR in the presence and absence of a defined DNA substrate. By doing so, we have succeeded in overcoming issues associated with high water absorbance to better monitor the peptide backbone region (1800–1600 cm^{-1}) of the CPD-PHR during the light-dependent repair process and identify unique features that distinguish CPD-PHR from its (6–4) counterpart.

MATERIALS AND METHODS

Enzyme Expression and Purification. The gene encoding *E. coli* CPD-PHR was inserted between the *Nde*I and *Xho*I sites of the pET-28a expression vector containing a His_6-tag in the upstream region of a multiple-cloning site (Novagen). E109A, which is a null mutant for MTHF binding,[17] was prepared by using QuikChange site-directed mutagenesis (Stratagene) according to standard protocols. Expression vectors were transformed into the *E. coli* BL21(DE3) strain (Stratagene). Cells were inoculated into 1 L of culture of Luria-Bertani medium in a 3 L flask and grown at 24 °C until the

dx.doi.org/10.1021/bi3016179 | *Biochemistry* 2013, 52, 1019–1027

OD_{660} reached 0.4, and IPTG was added to a final concentration of 1 mM. The culture was incubated at 18 °C for 18 h. Cells were harvested by centrifugation and stored at −80 °C. Cells were thawed on ice and resuspended in lysis buffer [50 mM NaH_2PO_4, 300 mM NaCl, 20 mM imidazole, and 5% (v/v) glycerol (pH 8.0)]. After sonication, the insoluble fraction was removed by centrifugation (17000*g*). The supernatant was loaded onto a Co-NTA column (TALON Metal Affinity Resin, Clontech); the column was washed using a 20-bed volume wash buffer [50 mM NaH_2PO_4, 300 mM NaCl, and 20 mM imidazole (pH 8.0)], and the fusion protein was eluted with elution buffer [50 mM NaH_2PO_4, 300 mM NaCl, and 250 mM imidazole (pH 8.0)]. Purified protein in elution buffer was then exchanged into storage buffer [50 mM HEPES, 100 mM NaCl, 10 mM β-mercaptoethanol, and 20% (v/v) glycerol (pH 7.0)] by dilution and ultrafiltration (Amicon Ultra 30K device, Millipore) prior to being stored at −80 °C. The majority of CPD-PHR resided in the semiquinone form during purification and measurement sample preparation. Notably, compared with (6−4) PHR, the oxidized form of the CPD-PHR enzyme was less efficiently photoreduced even in the presence of reducing agents as observed by our UV−vis and FTIR measurements described below. From 1 L of *E. coli* culture, approximately 6 and 12 mg of E109A and wild-type (WT) enzyme, respectively, were obtained.

Sample Preparation for UV−Vis and FTIR Measurement. The CPD module was synthesized and incorporated into double-stranded DNA for FTIR measurements according to the method described previously.[19] CPD was incorporated at the center (underlined) of the DNA oligonucleotide carrying the following sequence:

5′-CGCGAATTGCGCCC-3′
3′-GCGCTTAACGCGGG-5′

Unlike (6−4) PHR, the CPD-PHR sample complex was not amenable to the drying process required for FTIR measurements, as has also been found for *Synechocystis* Cry-DASH.[16] Instead, a concentrated aqueous CPD-PHR sample was used for this work. This method was developed on the basis of previous reports.[16,18] For FTIR measurements, the samples prepared in storage buffer were exchanged into FTIR measurement buffer [50 mM HEPES, 100 mM NaCl, 5% glycerol, and 25 mM β-mercaptoethanol (pH 7.0)]. Redissolved samples gave poor signals probably because of the instability of CPD-PHR with respect to drying. To facilitate the enzymatic activity during FTIR measurements, a higher water concentration was required. A compromise between retaining sufficient enzymatic activity and avoiding a strong IR water absorption was obtained by preparing CPD-PHR at high concentrations of approximately 2 mM. The sample concentration was determined from the absorbance of free FAD at 450 nm by UV−vis spectroscopy.

To measure CPD-PHR with its substrate at a 1:1 stoichiometric composition by FTIR, 1 μL of 2 mM CPD substrate in water was placed onto a BaF_2 window and dried until the volume of CPD reached approximately <0.5 μL. Subsequently, 1 μL of 2 mM CPD-PHR was added and the sample redried until the total volume became 1 μL, so that the salt concentration in the buffer remained approximately unchanged during sample preparation. A similar process was applied to generate a 1:2 enzyme:substrate stoichiometry. The samples were later sandwiched by another BaF_2 window and sealed with Parafilm.

For D_2O measurements, sample buffer was prepared using D_2O instead of H_2O. CPD-PHR was repeatedly diluted and concentrated with D_2O measurement buffer by ultrafiltration at 4 °C. The CPD substrate prepared in water was pipetted onto a BaF_2 window and vacuum-dried. The dried substrate was redissolved in 0.5 μL of D_2O prior to the addition of 1 μL of enzyme prepared in D_2O. The mixture was redried to 1 μL, sandwiched with another BaF_2 window, and sealed with Parafilm. All samples were prepared at room temperature and under ambient light conditions.

UV−Vis and FTIR Spectroscopy. UV−vis spectra were recorded with a V-550DS spectrometer (JASCO) equipped with an Optistat-DN (Oxford Instruments) cryostat mounted onto the spectrophotometer, which was also equipped with a temperature controller (ITC-4, Oxford Instruments). FTIR spectra were measured with a FTS-7000 instrument (DIGILAB) also equipped with an Optistat-DN cryostat and an ITC-4 temperature controller. The sample was illuminated with a 300 W xenon lamp (Max-302, ASAHI SPECTRA) with >550 and >390 nm filters. It should be noted that previous studies of (6−4) PHR were conducted using a 1 kW tungsten lamp in which the (6−4) PP repair reaction was completed in ∼20 min.[18] By contrast, the repair reaction of CPD-PHR in this study using a xenon lamp was completed within 3 min (data not shown).

RESULTS

Photoactivation and Photorepair of CPD-PHR Monitored by Light-Induced FTIR Spectroscopy. Previous reports showed that the MTHF cofactor binds loosely to *E. coli* CPD-PHR and was partially released upon purification.[20] We also detected weaker binding of MHTF following purification, as confirmed by the reduced absorbance at ∼380 nm upon illumination (Figure S1 of the Supporting Information). To facilitate sample homogeneity, we used the E109A mutant of CPD-PHR that lacks MTHF binding for our analysis; the E109A mutant can be still be photoreduced and has CPD repair activity similar to that of the wild-type (WT) enzyme.[21] The broad absorbance peak spreading between 500 and 700 nm is indicative of absorption by $FADH^{\bullet}$ (black line in Figure S1a of the Supporting Information). Illumination of E109A with >550 nm light resulted in reduced absorbance within this region, indicating that the enzyme was photoreduced from $FADH^{\bullet}$ to $FADH^{-}$ (red line in Figure S1a of the Supporting Information and dotted line in Figure S1c of the Supporting Information). The reducing ratio observed for E109A was comparable to that detected for WT CPD-PHR (solid lines in panels b and c of Figure S1 of the Supporting Information).

To elucidate the photorepair and photoactivation processes, light-induced difference FTIR spectroscopy was applied to CPD-PHR in the presence and absence of the DNA substrate carrying a single CPD. By using >550 and >390 nm light, photoactivation and photorepair reactions, respectively, can be discriminated in the sample.[16,18] Figure 2 shows light-induced difference FTIR spectra upon illumination at >550 nm (a) and subsequent illumination at >390 nm (b) in the absence (black lines) and presence (red lines) of double-stranded DNA carrying a CPD lesion. In the absence of damaged DNA, the observed spectrum simply shows the reduced-minus-semiquinone spectrum (Figure 2a, black line). Subsequent illumination of the sample with >390 nm light did not cause any spectral change (Figure 2b, black line), confirming that the

dx.doi.org/10.1021/bi3016179 | *Biochemistry* 2013, 52, 1019−1027

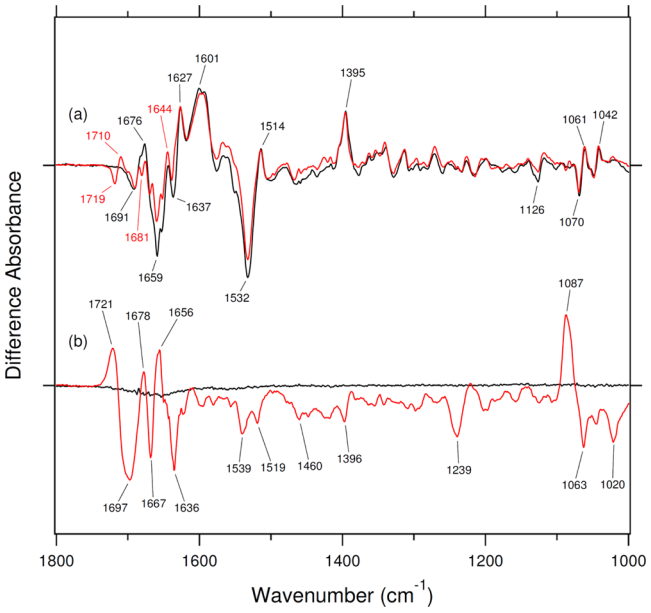

Figure 2. Light-induced difference FTIR spectra of CPD-PHR at 277 K showing photoactivation (a) and photorepair (b). The semiquinone enzyme with (red) and without (black) the CPD substrate was photoactivated by illumination with >550 nm light for 2 min. (b) Photoactivated enzyme with (red) and without (black) the CPD substrate was light-induced for photorepair by illumination with >390 nm light for 2 min. The enzyme:CPD molar ratio was 1:1. One division of the *y*-axis corresponds to 0.006 absorbance unit.

previous 2 min illumination with >550 nm light was sufficient for complete $FADH^{\bullet}$ reduction. Notably, the mutation from glutamate to alanine at amino acid position 109 with CPD-PHR did not perturb the photoactivation process (Figure S2 of the Supporting Information). Only slight differences in the amide I region (1670−1630 cm^{-1}) between WT and E109A enzymes could be observed, suggesting that even in the absence of MTHF, the photoactivation of E109A CDP-PHR proceeds as for the WT enzyme at this filtered wavelength and intensity.

In the presence of CPD substrate, illumination of PHR at >550 nm (Figure 2a, red line) gave a spectrum similar to that observed for the enzyme-minus-CPD spectrum (Figure 2a, black line). In contrast, an entirely different spectrum was obtained upon illumination with >390 nm light (Figure 2b, red line). For this measurement, PHR and damaged DNA were prepared at a 1:1 stoichiometry. More than 99% of the substrate is expected to bind the enzyme in darkness under these experimental conditions, as was estimated from the reported dissociation constant of 10^{-8} to 10^{-9} M for PHR and its substrate[10] (see Materials and Methods). Furthermore, with sufficient irradiation, the enzyme should be capable of repairing 100% of the CPD substrate and releasing the repaired DNA product under these experimental conditions (cf. Figure 4A in ref 18).

In the reduced-minus-semiquinone spectra of *E. coli* CPD-PHR (Figure 2a), the overall spectral shapes, including the characteristic peaks at 1532 (−) and 1395 (+) cm^{-1}, were consistent with those reported by Schleicher et al.[17] The negative peak at 1532 cm^{-1} can be attributed to ring I vibration and the N1═C10a stretching or N5−H bending mode from $FADH^{\bullet}$. The positive peak observed at 1395 cm^{-1} indicates the rocking mode of H5 from $FADH^{-}$.[17] While a UV-irradiated oligothymidine 18-mer was used in the previous report, our data using a defined CPD substrate showed slight but significant differences within the 1700−1600 cm^{-1} region with higher intensity. The bands in the 1700−1600 cm^{-1} region originate from the protein moiety as well as from C═O stretches of FAD ($FADH^{\bullet}$ and $FADH^{-}$ forms). The most prominent differences from both spectra in the presence and absence of the CPD substrate (Figure 2a) were found to be the peaks at 1719 (−)/1710 (+) cm^{-1}, which appeared only in the presence of substrate. The peaks in this region can be tentatively assigned to C═O stretches of a protonated carboxylic acid residue. To investigate this further, photoactivation of CPD-PHR was measured in the presence of the defined CPD substrate in D_2O (Figure 3a). The peaks observed

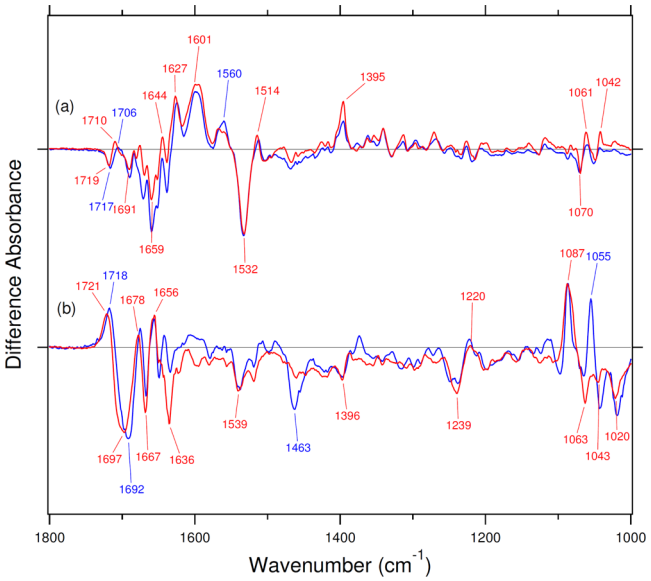

Figure 3. Light-induced difference FTIR spectra of CPD-PHR at 277 K showing photoactivation (a) and photorepair (b) in H_2O (red) and D_2O (blue). The carboxylic acid signal at 1719 (−) and 1710 (+) cm^{-1} (a) clearly showed downshifting during H−D exchange. One division of the *y*-axis corresponds to 0.006 absorbance unit.

at 1719 (−)/1710 (+) cm^{-1} in H_2O (red line) were shifted to 1717 (−)/1706 (+) cm^{-1} in D_2O (blue line), providing additional support for the idea that this pair of bands originates from a protonated carboxylic acid residue. A likely candidate responsible for these signals is glutamate at position 275, which located in the substrate-binding pocket of CPD-PHR,[22,23] although changes in C═O vibrations in the DNA substrate upon FAD reduction also cannot be ruled out. The relatively small shifts observed for these peaks may be due to limitations within our hydrogen−deuterium (H−D) exchange method. H−D sensitive spectral features above 1700 cm^{-1} were also observed for *Xenopus laevis* (6−4) PHR.[18] However, in CPD-PHR, the H−D change in the hydrogen bonding strength that we observed is the opposite of that measured for (6−4) PHR, and the peaks are at slightly lower frequencies; also, no carboxylic amino acid residue is present in the substrate-binding pocket of (6−4) PHR. Our findings identify FTIR features distinguishing the substrate binding step of the DNA repair processes by these respective PHRs, despite their commonalities.

The difference FTIR spectrum for the light-induced repair reaction of CPD-PHR exhibited strong peaks at 1721 (+), 1678 (+), 1239 (−), 1087 (+), and 1063 (+) cm^{-1} that most likely

dx.doi.org/10.1021/bi3016179 | *Biochemistry* 2013, 52, 1019−1027

originate from the repair and conversion of the CPD lesion back to two individual thymidine bases (Figure 2b, red line). To further decipher the origins of these peaks, a similar measurement was conducted in D_2O (Figure 3b, blue line). The band at 1721 (+) cm^{-1} likely corresponds to C4=O stretching of the recovered thymine moiety, while the peak at 1678 (+) cm^{-1} also likely originates from the C2=O stretch of the recovered thymine moiety,[24] as this peak is shifted during the D_2O measurements. Meanwhile, the negative peaks at 1460 and 1396 cm^{-1} are also likely to be derived from the conversion of CPD back to two pyrimidines as these absorbance peaks correspond to those reported previously.[17,25] Peaks at 1667 (−), 1656 (+), and 1636 (−) cm^{-1} did not shift following H−D exchange and presumably originate from the protein moiety. Antisymmetric and symmetric PO_2^- stretches of the DNA backbone are known to give rise to IR bands at ∼1230 and ∼1090 cm^{-1}, respectively.[17,18,25] Therefore, for CPD-PHR in the presence of DNA substrate, the paired peaks observed at 1239 (−) and 1221 (+) cm^{-1} can therefore be assigned as antisymmetric PO_2^- stretching and the paired peaks at 1087 (+) and 1063 (−) cm^{-1} as symmetric PO_2^- stretching of the DNA backbone.

Analysis of the Time Dependence of Photorepair by CPD-PHR. To assign major signals, we conducted FTIR spectroscopic measurements on the photoactivation and repair mechanisms of CPD-PHR at 1:1 enzyme:DNA substrate molar ratio. Under these conditions, however, we assumed that the spectra would also include information from the minor amount of free enzyme following substrate consumption. To exclude signals from free CPD-PHR, we next measured FTIR spectra in the presence of excess substrate. Consequently, we expected to improve the signal for the intermediate state of the CPD-PHR complex with the DNA substrate, as was observed in a previous (6−4) PHR study.[18] Early sampling should give signals dominated by the complex, while later sampling should more closely match signals from conditions with a 1:1 stoichiometry (see a more detailed concept in ref 18). Subsequent time-dependent measurements were therefore performed at a 1:2 enzyme:DNA substrate stoichiometry.

Illumination of CPD-PHR and DNA substrate with >550 nm light, followed by illumination with >390 nm light, was conducted every 20 s. The spectra obtained after the initial 20 s gave the strongest spectral intensities. These intensities diminished upon prolonged illumination up to 140 s (Figure S3 of the Supporting Information). Double-stranded DNA substrate containing the CPD lesion was completely repaired within 140 s and showed no significant spectral change upon further illumination. After illumination for 140 s, the peak intensities of the spectra obtained with a 1:2 enzyme:substrate molar ratio were approximately 2-fold higher than those obtained for a 1:1 molar ratio.

The overall spectra obtained for the enzyme−substrate sample prepared at a 1:1 molar ratio remained largely unchanged between early (0−20 s) and late (80−100 s) stages of illumination (data not shown). In contrast, some significant changes could be observed between early and late stages in the spectra obtained for samples with 1:2 enzyme:substrate molar ratios (Figure 4a, black and red lines, respectively). When normalized at 1721 cm^{-1}, the late spectra gain new positive signals at 1656 and 1645 cm^{-1} and more intense signals at 1678 (+), 1241 (−), and 1087 (+) cm^{-1}. These trends imply formation of a new spectral species or one state whose amount increases significantly from the early to late stages of

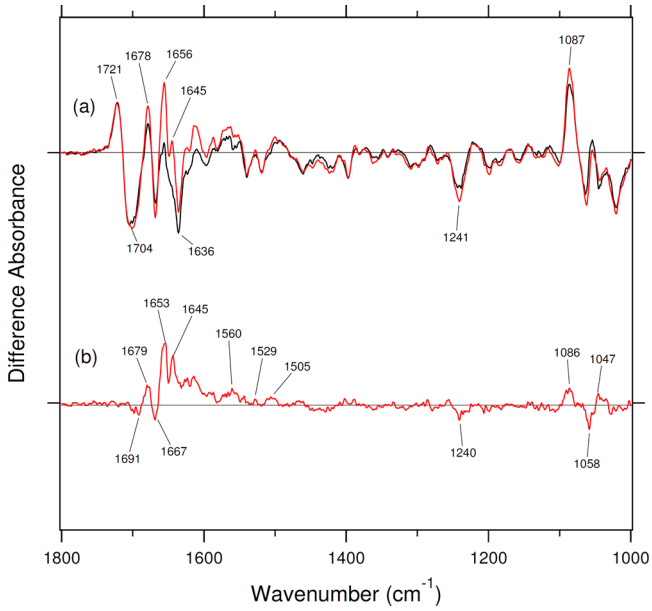

Figure 4. FTIR spectral comparison between early (0−20 s, black) and late (80−100 s, red) stages of illumination for the 1:2 enzyme:substrate molar ratio (a), with the red line scaled up 5-fold for normalization. Double-difference spectra between the early and late stages of part a are shown in part b.

illumination. The early stage spectra more closely resemble those obtained in a previous report about CPD-PHR.[17] Some differences observed between the two sets of experiments may result from the different DNA substrates and enzyme:substrate stoichiometries used. In this study, we used a defined DNA oligonucleotide carrying a single CPD, whereas the previous FTIR study employed an oligothymidine 18-mer substrate generated by UV irradiation. The UV-irradiated polythymidine could contain multiple CPDs within the DNA duplex, which could increase the available amount of CPD substrate to more closely resemble the 1:2 enzyme:substrate molar ratio used in our study.

Subtraction of spectra between late and early stages, as shown in Figure 4b, gives a representation of the conformational rearrangements occurring within the enzyme−substrate complex. The peaks in the 1800−1500 cm^{-1} range are likely amide I and II signals, indicating conformational changes in the enzyme's polypeptide backbone, most likely rearrangements of the α-helices in or near the binding site for damaged DNA substrate. Perturbations of the ring moiety of the CPD substrate upon enzyme binding could also generate FTIR signals in this range. Peaks at 1240 (−) and 1086 (+) cm^{-1} should originate from changes in the DNA phosphate backbone vibrations due to the dinucleotide flipping and further bending of the DNA helix, which are induced by the CPD-PHR during substrate recognition and binding, respectively (Figure 4b).

DISCUSSION

FTIR Assignments of the DNA Backbone Controlled by PHRs. In this study, we have successfully measured FTIR signals generated from the repair of a single CPD lesion within a double-stranded DNA molecule by *E. coli* CPD-PHR and compared the results to a previous study[18] of (6−4) PP lesion photorepair by (6−4) PHR. From the findings presented here, we detected several new features unique to the CPD-PHR photoactivation and repair process. In contrast to a previous

dx.doi.org/10.1021/bi3016179 | *Biochemistry* 2013, 52, 1019−1027

FTIR report about *E. coli* CPD-PHR,[17] which detected an FTIR peak at 1224 cm^{-1} during repair of a UV-irradiated oligodeoxythymidine 18-mer, we instead observed peaks at 1240 (−) and 1086 (+) cm^{-1} (Figure 4b), which occur when the enzyme binds to its DNA substrate. These peaks most likely originate from perturbations of the DNA phosphate backbone.

For better elucidation of the photorepair process by PHRs, the light-dependent DNA repair of CPD-PHR was compared to that of (6–4) PHR. In the both experiments, 2 and 4 μmol of damaged DNA were used in the 1:1 and 1:2 stoichiometric compositions, respectively, of the PHRs (see Materials and Methods). Although the starting damaged DNA substrates were different, both repairs produced an identical product, two normal thymidines. Thus, we expected similar positive peaks of comparable intensity derived from the products generated from the DNA repair spectra obtained from two different PHRs. Figure S4 of the Supporting Information compares the repair spectra of CPD and (6–4) photoproducts by their respective PHRs without any modifications. Intensities of the peaks at <1400 cm^{-1} look similar between the two spectra. Therefore, we concluded that these two independent experiments give similar intensities regarding the reaction products generated and assumed that the positive peak at ∼1086 cm^{-1} could be used as a marker band for normalization between CPD and (6–4) PP repair spectra.

Figure 5a compares early stages of time dependence spectra of both CPD-PHR (black line) and (6–4) PHR (red line)

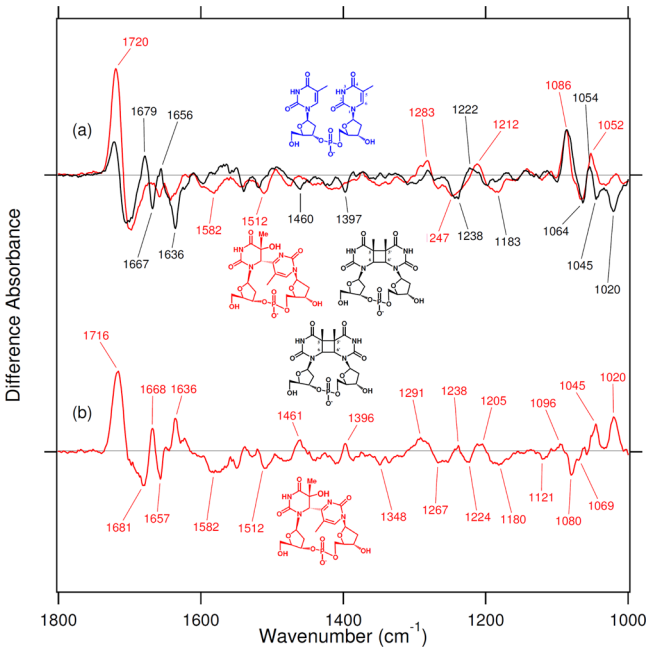

Figure 5. (a) Superimposition of light-induced FTIR difference spectra of PPs treated with the respective PHRs: (6–4) PP by (6–4) PHR (red) and CPD by CPD-PHR (black). (b) Double-difference spectrum between CPD and (6–4) PP repair showing distinct DNA backbone rearrangements by PHRs. One division of the *y*-axis corresponds to 0.004 absorbance unit.

normalized for the peak at 1086 cm^{-1}. When we subtract the red signals [normal intact DNA minus (6–4) PP] from the black signals (normal intact DNA minus CPD) in Figure 5a, the difference yields a FTIR difference spectrum [CPD minus (6–4) PP] (Figure 5b). In this spectrum, the positive and negative bands correspond to CPD and (6–4) PP, respectively. The peak at 1720 cm^{-1} represents the vibration of the C4═O group of thymidines.[18] In the repair spectra of (6–4) PHR, this signal shows higher intensity due to the new formation of the C4═O group at the 3′-side of adjacent pyrimidines. We also observe some common characteristic bands; bands at 1238 (−)/1222 (+) cm^{-1} (black line) and 1247 (−)/1212 (+) cm^{-1} (red line) arise from antisymmetric vibration of the DNA phosphate backbone, while peaks at 1086 (+), 1064 (−), 1054 (+) cm^{-1} (black line) and 1086 (+), 1064 (−), and 1052 (+) cm^{-1} (red line) show symmetric vibration of the DNA phosphate backbone. As shown by crystallographic studies, both CPD-PHR and (6–4) PHRs kink the damaged DNA by dinucleotide flipping and then release the restored DNA. These positive peaks indicate that rearrangements of the damaged DNA substrate backbone to the B-DNA conformation can be detected, allowing us to assign major peaks.

Comparison of Two PHRs in Their Substrate Recognition Modes. Figure 6 compares the spectrum of CPD-PHR

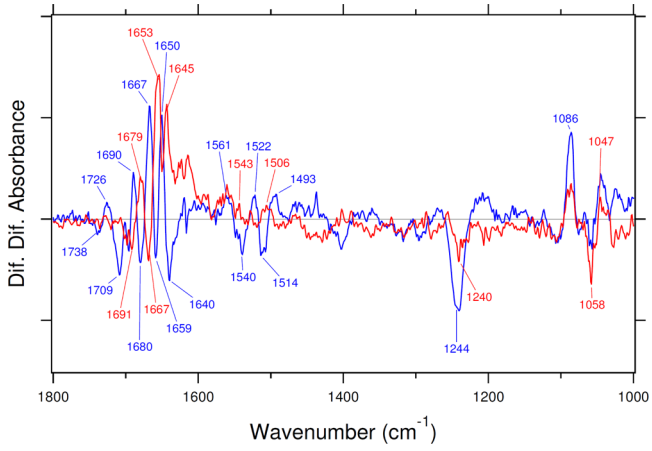

Figure 6. Superimposition of light-induced FTIR difference spectra for photorepair by (6–4) PHR (blue) and by CPD-PHR (red) reveals distinct α-helical rearrangements within the protein fold. One division of the *y*-axis corresponds to 0.001 absorbance unit.

(red line, this study) with that of (6–4) PHR (blue line, reproduced from ref 18) at the initial stage dominated by the PHR–substrate complex (also see Figure 1a). After the two spectra were normalized at 1086 cm^{-1} for quantitative comparison, larger structural changes in the phosphate PO^{-} stretches were observed for the (6–4) PP than for the CPD lesion. The (6–4) PP induces severe distortion of the DNA (Figure 1b,c), whereas a DNA oligonucleotide carrying a single CPD is much closer in conformation to B-DNA (Figure 1b,c).[26] (6–4) PHRs may expend energy for induced fitting of the substrate within the active site, whereas this may not be necessary for CPD-PHRs. If a hydrogen bond from a carboxylic acid group is modified with the change in the redox status of the FAD cofactor or during DNA repair, a resulting FTIR signal would be expected to appear in the 1750–1700 cm^{-1} region. *E. coli* CPD-PHR does not produce a significant signal within this region, unlike *Xenopus* (6–4) PHR. This findings lead to two possible alternatives for CPD-PHR substrate recognition. First, a hydrogen bond network including a carboxylic acid residue in the DNA-binding pocket of CPD-PHR may be changed upon substrate binding. A second possibility could result from the DNA substrate itself, whereby the C4═O vibration from the thymine moiety is shifted by a change in the FAD redox status.

dx.doi.org/10.1021/bi3016179 | *Biochemistry* 2013, 52, 1019–1027

All light-dependent repair reactions of damaged DNA by PHR are triggered by the reduction of the FAD. The correlation between the FAD redox state and C4=O vibration in the DNA substrate is also intriguing. However, future studies, such as mutagenesis and isotope labeling of enzymes and substrates, are required to determine these underlying differences in the FTIR signals obtained for (6–4) PHR and CPD-PHR.

In the amide I region, most of the peaks obtained for CPD-PHR and (6–4) PHR were opposite (+ vs −) to each other, showing conformational differences between these enzymes in their substrate recognition mode. The 1650 cm^{-1} region represents α-helix changes. Differences within this region therefore suggest that the two enzymes exhibit distinct α-helical rearrangements upon substrate binding.

To improve our understanding of the conformational dynamics of PHR substrate recognition identified by FTIR, we superimposed crystal structures of CPD-PHR [from *Aspergillus nidulans*, Protein Data Bank (PDB) entry 1TEZ][23] and (6–4) PHR (from *Drosophila melanogaster*, PDB entry 3CVV)[27] bound with their respective DNA substrates (Figure 7). Both enzymes show similar overall structures, consisting of two major domains: N-terminal α/β and C-terminal α-helical domains, connected by a long loop. The active site cavity, specific to each PP substrate, is located adjacent to the redox active FAD cofactor in the C-terminal α-helical domain. Thus, the distinctive α-helical FTIR signals likely arise from this region that interacts with the substrate. Notably, the overlaid structures show more structural rearrangements in the α-helices that pinch the damaged DNA photoproduct (circled in Figure 7) and interface with the complementary DNA strand than in the rest of the domain. The foundation helix of the "FAD triangle" of helices framing the FAD binding cavity (for the nomenclature, see ref 28) packs against 3′-side of the photoproduct, while the C-terminal helix is used as an interface for the complementary strand. In the DNA duplex, CPD and (6–4) photoproducts show different structural features at the 3′-base rather than at the 5′-base, which retains Watson–Crick base pair sites (Figure 1b,c). Moreover, different PHRs show distinctive structural features in the region fitting to the 3′-side of photoproduct even without the substrate; (6–4) PHR partially constricts the entrance to the substrate cavity with a 3_{10}-helix and gains an extra interaction with FAD, whereas CPD-PHRs do not have such a structural feature.[29] Together with our FTIR observations, these data indicate that PHRs uniquely utilize these α-helices to flip out of the DNA duplex and fit their respective photoproduct substrates into the cavity.

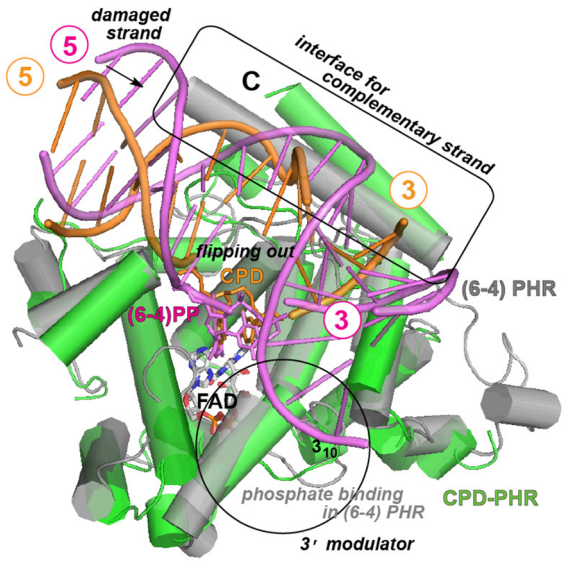

Figure 7. Overlaid PHR (substrate-binding α-helical barrel domain) structures indicate distinctive active site conformations appropriate for recognizing and repairing the divergent 3′-side of their respective PP substrates (also see Figure 1b,c). CPD-PHR is colored green and DNA carrying CPD orange; (6–4) PHR and DNA with (6–4) PP are colored gray and violet, respectively. FAD and PP at the active sites are presented as sticks. CPD-PHR aligns a 3_{10}-helix at the active site to pinch the 3′-side of PP (circle, 3′-modulator), whereas (6–4) PHRs conserve a phosphate-binding motif. Both enzymes utilize a long helix in the C-terminus (box) as an interface for the complementary undamaged DNA strand.

To test this conclusion, we mapped crystallographic temperature factors (*B* values) onto the structures of CPD-PHRs from *E. coli* (PDB entry 1DNP)[22] and *A. nidulans* without (PDB entry 1QNF)[30] and with their bound DNA substrates (PDB entry 1TEZ) as models for CPD-PHRs (Figure S5 of the Supporting Information). Despite the different origins and crystallization conditions for these structures, *B* value mapping indicates flexibility for rearranging helices to fit against the 3′-side of the CPD photoproduct and to interact with the complementary DNA strand. Moreover, structural superpositions of the unbound *A. nidulans* CPD-PHR (PDB entry 1QNF) and its DNA complex (PDB entry 1TEZ) show few differences within the polypeptide backbone; however, a 3_{10}-helix in the region is significantly shifted. Structures of the substrate-free forms of *E. coli* and *A. nidulans* CPD-PHRs also differ slightly in this region. The 3_{10}-helix is not well-defined in the substrate-free *E. coli* enzyme structure, probably because of its flexibility. Similarly, comparison of the *A. nidulans* CPD-PHR structures implies that this flexible region gains rigidity upon binding the damaged DNA substrate. Thus, analysis of *B* value mapping and structural superpositions support our FTIR conclusions linking protein backbone flexibility to distinct helical rearrangements during substrate recognition and repair by different PHRs.

In conclusion, we have successfully employed FTIR spectroscopy to monitor the light-dependent repair reaction of *E. coli* CPD-PHR by using a well-defined DNA substrate. Despite the high concentration of water required for CPD-PHR enzymatic turnover in vitro, we were successful in concentrating samples suitable for FTIR studies. Consequently, novel peaks within the peptide backbone region of CPD-PHR were detected, and major signals arising during the DNA repair process were assigned. By comparing FTIR results for CPD-PHR and (6–4) PHR, which repair UV-damaged DNA photoproducts with different linkages, we found that these PHRs employ distinct α-helical rearrangements within their substrate binding sites allowing each to specifically recognize and repair its own substrate. These different dynamics in protein flexibility provide a molecular framework for understanding how PHRs can share a common overall structural fold yet selectively identify the correct photoproduct within a damaged DNA duplex.

■ ASSOCIATED CONTENT

Supporting Information

UV–visible absorption spectra of WT and E109A CPD-PHRs (Figure S1), reduced-minus-semiquinone FTIR difference spectra of E109A and WT CPD-PHRs (Figure S2), time-

dx.doi.org/10.1021/bi3016179 | *Biochemistry* 2013, 52, 1019–1027

dependent spectra of illumination for the 1:2 enzyme−substrate mixtures in the 1800−1000 cm^{-1} region (Figure S3), photorepair spectra of CPD and (6−4) PP for the 1:1 and 1:2 mixtures (Figure S4), and crystal structure comparisons of the (a) *E. coli* (PDB entry 1DNP) and (b) *A. nidulans* (PDB entry 1QNF) CPD-PHR enzymes together with the (c) enzyme−DNA substrate complex from *A. nidulans* (PDB entry 1TEZ) and superimpositions of (d) CPD-PHR from *E. coli* (PDB entry 1DNP) and *A. nidulans* (PDB entry 1QNF) and (e) CPD-PHR from *A. nidulans* with and without the DNA substrate (Figure S5). This material is available free of charge via the Internet at http://pubs.acs.org.

AUTHOR INFORMATION

Corresponding Author

*Department of Frontier Materials, Nagoya Institute of Technology, Showa-ku, Nagoya 466-8555, Japan. Phone and fax: 81-52-735-5207. E-mail: kandori@nitech.ac.jp.

Notes

The authors declare no competing financial interest.

ACKNOWLEDGMENTS

We are grateful to Dr. John M. Christie for useful discussion and careful reading of the manuscript.

ABBREVIATIONS

PHR, photolyase; CPD, cyclobutane pyrimidine dimer; FAD, flavin adenine dinucleotide; $FADH^-$, reduced form of FAD; $FADH^•$, semiquinoid form of FAD; H−D exchange, hydrogen−deuterium exchange; MTHF, 5,10-methylenetetrahydrofolate; PP, photoproduct; FTIR, Fourier transform infrared; UV−vis, ultraviolet−visible.

REFERENCES

(1) Sinha, R. P., and Hader, D. P. (2002) UV-induced DNA damage and repair: A review. *Photochem. Photobiol. Sci. 1*, 225−236.

(2) Douki, T., Reynaud-Angelin, A., Cadet, J., and Sage, E. (2003) Bipyrimidine photoproducts rather than oxidative lesions are the main type of DNA damage involved in the genotoxic effect of solar UVA radiation. *Biochemistry 42*, 9221−9226.

(3) Friedberg, E. C., Walker, G. C., Siede, W., Wood, R. D., Schultz, R. A., and Ellenberger, T. (2006) *DNA repair and mutagenesis*, 2nd ed., Elsevier, Amsterdam.

(4) Sertic, S., Pizzi, S., Lazzaro, F., Plevani, P., and Muzi-Falconi, M. (2012) NER and DDR: Classical music with new instruments. *Cell Cycle 11*, 668−674.

(5) Waters, L. S., Minesinger, B. K., Wiltrout, M. E., D'Souza, S., Woodruff, R. V., and Walker, G. C. (2009) Eukaryotic Translesion Polymerases and Their Roles and Regulation in DNA Damage Tolerance. *Microbiol. Mol. Biol. Rev. 73*, 134−154.

(6) Sancar, A., and Sancar, G. B. (1984) *Escherichia coli* DNA photolyase is a flavoprotein. *J. Mol. Biol. 172*, 223−227.

(7) Todo, T., Kim, S. T., Hitomi, K., Otoshi, E., Inui, T., Morioka, H., Kobayashi, H., Ohtsuka, E., Toh, H., and Ikenaga, M. (1997) Flavin adenine dinucleotide as a chromophore of the *Xenopus* (6−4) photolyase. *Nucleic Acids Res. 25*, 764−768.

(8) Jorns, M. S., Sancar, G. B., and Sancar, A. (1984) Identification of a neutral flavin radical and characterization of a second chromophore in *Escherichia coli* DNA photolyase. *Biochemistry 23*, 2673−2679.

(9) Payne, G., Heelis, P. F., Rohrs, B. R., and Sancar, A. (1987) The active form of *Escherichia coli* DNA photolyase contains a fully reduced flavin and not a flavin radical, both in vivo and in vitro. *Biochemistry 26*, 7121−7127.

(10) Kim, S. T., and Sancar, A. (1993) Photochemistry, photophysics, and mechanism of pyrimidine dimer repair by DNA photolyase. *Photochem. Photobiol. 57*, 895−904.

(11) Byrdin, M., Eker, A. P., Vos, M. H., and Brettel, K. (2003) Dissection of the triple tryptophan electron transfer chain in *Escherichia coli* DNA photolyase: Trp382 is the primary donor in photoactivation. *Proc. Natl. Acad. Sci. U.S.A. 100*, 8676−8681.

(12) Berg, B. J. V., and Sancar, G. B. (1998) Evidence for dinucleotide flipping by DNA Photolyase. *J. Biol. Chem. 32*, 20276−20284.

(13) Siebert, F. (1995) Infrared spectroscopy applied to biochemical and biological problems. *Methods Enzymol. 246*, 501−526.

(14) Masuda, S., Hasegawa, K., Ishii, A., and Ono, T. A. (2004) Light-induced structural changes in a putative blue-light receptor with a novel FAD binding fold sensor of blue-light using FAD (BLUF); Slr1694 of *Synechocystis sp*. PCC 6803. *Biochemistry 43*, 5304−5313.

(15) Iwata, T., Nozaki, D., Tokutomi, S., Kagawa, T., Wada, M., and Kandori, H. (2003) Light-induced structural changes in the LOV2 domain of *Adiantum phytochrome3* studied by low-temperature FTIR and UV-visible spectroscopy. *Biochemistry 42*, 8183−8191.

(16) Iwata, T., Zhang, Y., Hitomi, K., Getzoff, E. D., and Kandori, H. (2010) Key dynamics of conserved asparagine in a cryptochrome/photolyase family protein by Fourier transform infrared spectroscopy. *Biochemistry 49*, 8882−8891.

(17) Schleicher, E., Hessling, B., Illarionova, V., Bacher, A., Weber, S., Richter, G., and Gerwert, K. (2005) Light-induced reactions of *Escherichia coli* DNA photolyase monitored by Fourier transform infrared spectroscopy. *FEBS J. 272*, 1855−1866.

(18) Zhang, Y., Iwata, T., Yamamoto, J., Hitomi, K., Iwai, S., Todo, T., Getzoff, E. D., and Kandori, H. (2011) FTIR study of light-dependent activation and DNA repair processes of (6−4) photolyase. *Biochemistry 50*, 3591−3598.

(19) Murata, T., Iwai, S., and Ohtsuka, E. (1990) Synthesis and characterization of a substrate for T4 endonuclease V containing a phosphorodithioate linkage at the thymine dimer site. *Nucleic Acids Res. 18*, 7279−7286.

(20) Hamm-Alvarez, S., Sancar, A., and Rajagopalan, K. V. (1990) The folate cofactor of *Escherichia coli* DNA photolyase acts catalytically. *J. Biol. Chem. 265*, 18656−18662.

(21) Jorns, M. S., Wang, B. Y., Jordan, S. P., and Chanderkar, L. P. (1990) Chromophore function and interaction in *Escherichia coli* DNA photolyase: Reconstitution of the apoenzyme with pterin and/or flavin derivatives. *Biochemistry 29*, 552−561.

(22) Park, H. W., Kim, S. T., Sancar, A., and Deisenhofer, J. (1995) Crystal structure of DNA photolyase from *Escherichia coli*. *Science 268*, 1866−1872.

(23) Mees, A., et al. (2004) Crystal structure of a photolyase bound to a CPD-like DNA lesion after in situ repair. *Science 306*, 1789−1793.

(24) Hernandez, B., Navarro, R., Vergoten, G., and Hernanz, A. (2001) Ab initio vibrational calculations on ara-T molecule: Application to analysis of IR and Raman spectra. *Biopolymers 62*, 193−207.

(25) Taillandier, E., and Liquier, J. (1992) Infrared spectroscopy of DNA. *Methods Enzymol. 211*, 307−335.

(26) McAteer, K., Jing, Y., Kao, J., Taylor, J. S., and Keneddy, M. A. (1998) Solution-state structure of a DNA dodecamer duplex containing a Cis-syn thymine cyclobutane dimer, the major UV photoproduct of DNA. *J. Mol. Biol. 282*, 1013−1032.

(27) Glas, A. F., Maul, M. J., Cryle, M., Barends, T. R., Schneider, S., Kaya, E., Schlichting, I., and Carell, T. (2009) The archaeal cofactor F0 is a light-harvesting antenna chromopore in eukaryotes. *Proc. Natl. Acad. Sci. U.S.A. 106*, 11540−11545.

(28) Hitomi, K., Arvai, A. S., Yamamoto, J., Hitomi, C., Teranishi, M., Hirouchi, T., Yamamoto, K., Iwai, S., Tainer, J. A., Hidema, J., and Getzoff, E. D. (2012) Eukaryotic class II cyclobutane pyrimidine dimer photolyase structure reveals basis for improved ultraviolet tolerance in plants. *J. Biol. Chem. 287*, 12060−12069.

(29) Hitomi, K., DiTacchio, L., Arvai, A. S., Yamamoto, J., Kim, S. T., Todo, T., Tainer, J. A., Iwai, S., Panda, S., and Getzoff, E. D. (2009)

Functional motifs in the (6−4) photolyase crystal structure make a comparative framework for DNA repair photolyases and clock cryptochromes. *Proc. Natl. Acad. Sci. U.S.A. 106*, 6962−6967.
(30) Tamada, T., Kitadokoro, K., Higuchi, Y., Inaka, K., Yasui, A., de Ruiter, P. E., Eker, A. P., and Miki, K. (1997) Crystal structure of DNA photolyase from *Anacystis nidulans*. *Nat. Struct. Biol. 11*, 887−891.